



E-ISSN: 2708-454X
 P-ISSN: 2708-4531
 IJRCDS 2021; 2(2): 77-86
 © 2021 IJRCDS
www.circuitsjournal.com
 Received: 20-05-2021
 Accepted: 22-06-2021

EL Pankratov

- a) Nizhny Novgorod State University, 23 Gagarin avenue, Nizhny Novgorod, 603950, Russia
 b) Nizhny Novgorod State Technical University, 24 Minin Street, Nizhny Novgorod, 603950, Russia

Correspondence

EL Pankratov

- a) Nizhny Novgorod State University, 23 Gagarin avenue, Nizhny Novgorod, 603950, Russia
 b) Nizhny Novgorod State Technical University, 24 Minin Street, Nizhny Novgorod, 603950, Russia

On increasing of density of elements of a differential-drive CMOS heterorectifier. On influence of mismatch-induced stress and porosity of materials on technological process

EL Pankratov

Abstract

In this paper we introduce an approach to increase density of field-effect transistors in the framework of a differential-drive CMOS rectifier. Framework the approach we consider manufacturing the rectifier in heterostructure with specific configuration. Several required areas of the heterostructure should be doped by diffusion or ion implantation. After that dopant and radiation defects should be annealed framework optimized scheme. We also consider an approach to decrease value of mismatch-induced stress in the considered heterostructure. We introduce an analytical approach to analyze mass and heat transport in heterostructures during manufacturing of integrated circuits with account mismatch-induced stress.

Keywords: Differential-drive CMOS rectifier, optimization of manufacturing, accounting of mismatch-induced stress and porosity of materials; analytical approach for modelling

Introduction

In the present time several actual problems of the solid state electronics (such as increasing of performance, reliability and density of elements of integrated circuits: diodes, field-effect and bipolar transistors) are intensively solving [1-6]. To increase the performance of these devices it is attracted an interest determination of materials with higher values of charge carriers mobility [7-10]. One way to decrease dimensions of elements of integrated circuits is manufacturing them in thin film heterostructures [3-5, 11]. In this case it is possible to use inhomogeneity of heterostructure and necessary optimization of doping of electronic materials [12] and development of epitaxial technology to improve these materials (including analysis of mismatch induced stress) [13-15]. An alternative approaches to increase dimensions of integrated circuits are using of laser and microwave types of annealing [16-18].

Framework the paper we introduce an approach to manufacture field-effect transistors. The approach gives a possibility to decrease their dimensions with increasing their density framework a differential-drive CMOS rectifier. We also consider possibility to decrease mismatch-induced stress to decrease quantity of defects, generated due to the stress. In this paper we consider a heterostructure, which consist of a substrate and an epitaxial layer (see Fig. 1). We also consider a buffer layer between the substrate and the epitaxial layer. The epitaxial layer includes into itself several sections, which were manufactured by using another materials. These sections have been doped by diffusion or ion implantation to manufacture the required types of conductivity (p or n). These areas became sources, drains and gates (see Fig. 1). After this doping it is required annealing of dopant and/or radiation defects. Main aim of the present paper is analysis of redistribution of dopant and radiation defects to determine conditions, which correspond to decreasing of elements of the considered rectifier and at the same time to increase their density. At the same time we consider a possibility to decrease mismatch-induced stress.

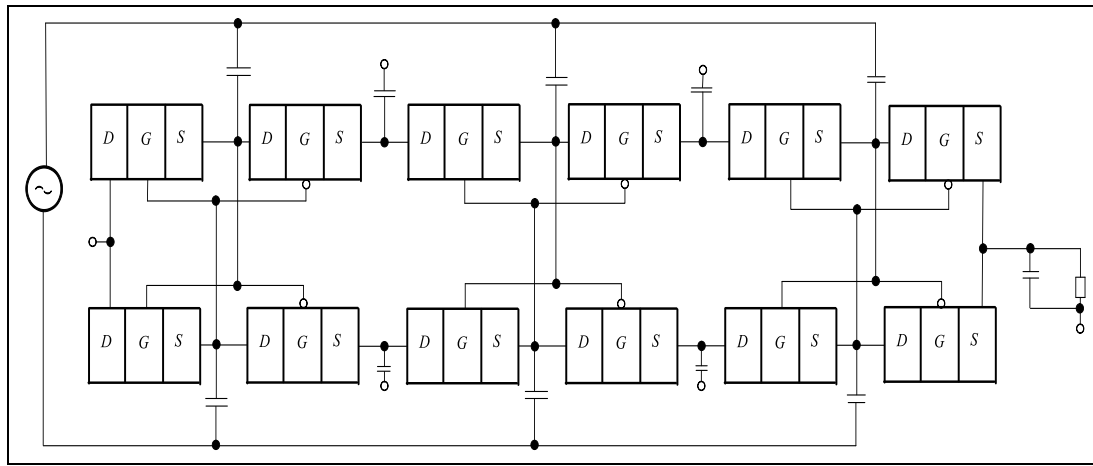


Fig 1a: Structure of the considered rectifier [19].

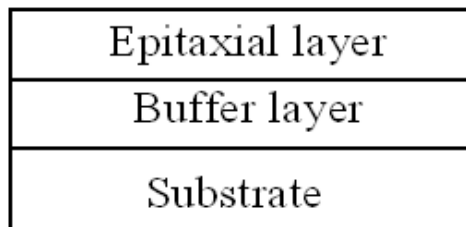


Fig 1b: Heterostructure with a substrate, epitaxial layers and buffer layer (view from side)

Method of Solution

To solve our aim we determine and analyzed spatio-temporal distribution of concentration of dopant in the considered heterostructure. We determine the distribution by solving the second Fick's law in the following form [1, 20-23].

$$\begin{aligned} \frac{\partial C(x, y, z, t)}{\partial t} &= \frac{\partial}{\partial x} \left[D \frac{\partial C(x, y, z, t)}{\partial x} \right] + \frac{\partial}{\partial y} \left[D \frac{\partial C(x, y, z, t)}{\partial y} \right] + \frac{\partial}{\partial z} \left[D \frac{\partial C(x, y, z, t)}{\partial z} \right] + \\ &+ \Omega \frac{\partial}{\partial x} \left[\frac{D_s}{kT} \nabla_s \mu_1(x, y, z, t) \int_0^{L_z} C(x, y, W, t) dW \right] + \\ &+ \Omega \frac{\partial}{\partial y} \left[\frac{D_s}{kT} \nabla_s \mu_1(x, y, z, t) \int_0^{L_z} C(x, y, W, t) dW \right] + \\ &+ \frac{\partial}{\partial x} \left[\frac{D_{cs}}{\bar{V} kT} \frac{\partial \mu_2(x, y, z, t)}{\partial x} \right] + \frac{\partial}{\partial y} \left[\frac{D_{cs}}{\bar{V} kT} \frac{\partial \mu_2(x, y, z, t)}{\partial y} \right] + \frac{\partial}{\partial z} \left[\frac{D_{cs}}{\bar{V} kT} \frac{\partial \mu_2(x, y, z, t)}{\partial z} \right] \end{aligned} \tag{1}$$

with boundary and initial conditions

$$\begin{aligned} \left. \frac{\partial C(x, y, z, t)}{\partial x} \right|_{x=0} &= 0, \left. \frac{\partial C(x, y, z, t)}{\partial x} \right|_{x=L_x} &= 0, \left. \frac{\partial C(x, y, z, t)}{\partial y} \right|_{y=0} &= 0, C(x, y, z, 0) = f_C(x, y, z), \\ \left. \frac{\partial C(x, y, z, t)}{\partial y} \right|_{x=L_y} &= 0, \left. \frac{\partial C(x, y, z, t)}{\partial z} \right|_{z=0} &= 0, \left. \frac{\partial C(x, y, z, t)}{\partial z} \right|_{x=L_z} &= 0. \end{aligned}$$

Here $C(x, y, z, t)$ is the spatio-temporal distribution of concentration of dopant; Ω is the atomic volume of dopant; ∇_s is the symbol of surficial gradient; $\int_0^{L_z} C(x, y, z, t) dz$ is the surficial concentration of dopant on interface between layers of heterostructure (in this situation we assume, that Z-axis is perpendicular to interface between layers of heterostructure);

$\mu_1(x,y,z,t)$ and $\mu_2(x,y,z,t)$ are the chemical potential due to the presence of mismatch-induced stress and porosity of material; D and D_S are the coefficients of volumetric and surficial diffusions. Values of dopant diffusions coefficients depends on properties of materials of heterostructure, speed of heating and cooling of materials during annealing and spatio-temporal distribution of concentration of dopant. Dependences of dopant diffusions coefficients on parameters could be approximated by the following relations [24-26].

$$D_C = D_L(x, y, z, T) \left[1 + \xi \frac{C^\gamma(x, y, z, t)}{P^\gamma(x, y, z, T)} \right] \left[1 + \zeta_1 \frac{V(x, y, z, t)}{V^*} + \zeta_2 \frac{V^2(x, y, z, t)}{(V^*)^2} \right],$$

$$D_S = D_{SL}(x, y, z, T) \left[1 + \xi_S \frac{C^\gamma(x, y, z, t)}{P^\gamma(x, y, z, T)} \right] \left[1 + \zeta_1 \frac{V(x, y, z, t)}{V^*} + \zeta_2 \frac{V^2(x, y, z, t)}{(V^*)^2} \right]. \quad (2)$$

Here $D_L(x,y,z,T)$ and $D_{LS}(x,y,z,T)$ are the spatial (due to accounting all layers of heterostructure) and temperature (due to Arrhenius law) dependences of dopant diffusion coefficients; T is the temperature of annealing; $P(x,y,z,T)$ is the limit of solubility of dopant; parameter γ depends on properties of materials and could be integer in the following interval $\gamma \in [1, 3, 24]$; $V(x,y,z,t)$ is the spatio-temporal distribution of concentration of radiation vacancies; V^* is the equilibrium distribution of vacancies. Concentrational dependence of dopant diffusion coefficient has been described in details in [24]. Spatio-temporal distributions of concentration of point radiation defects have been determined by solving the following system of equations [20-23, 25, 26].

$$\begin{aligned} \frac{\partial \rho(x, y, z, t)}{\partial t} = & \frac{\partial}{\partial x} \left[D_\rho(x, y, z, T) \frac{\partial \rho(x, y, z, t)}{\partial x} \right] + \frac{\partial}{\partial y} \left[D_\rho(x, y, z, T) \frac{\partial \rho(x, y, z, t)}{\partial y} \right] + \\ & + \frac{\partial}{\partial z} \left[D_\rho(x, y, z, T) \frac{\partial \rho(x, y, z, t)}{\partial z} \right] - k_{\rho,\rho}(x, y, z, T) \rho^2(x, y, z, t) - k_{I,V}(x, y, z, T) \times \\ & \times I(x, y, z, t) V(x, y, z, t) + \Omega \frac{\partial}{\partial x} \left[\frac{D_{\rho S}}{kT} \nabla_s \mu(x, y, z, t) \int_0^{L_z} \rho(x, y, W, t) dW \right] + \\ & + \Omega \frac{\partial}{\partial y} \left[\frac{D_{\rho S}}{kT} \nabla_s \mu(x, y, z, t) \int_0^{L_z} \rho(x, y, W, t) dW \right] + \frac{\partial}{\partial x} \left[\frac{D_{\rho S}}{\bar{V} kT} \frac{\partial \mu_2(x, y, z, t)}{\partial x} \right] + \\ & + \frac{\partial}{\partial y} \left[\frac{D_{\rho S}}{\bar{V} kT} \frac{\partial \mu_2(x, y, z, t)}{\partial y} \right] + \frac{\partial}{\partial z} \left[\frac{D_{\rho S}}{\bar{V} kT} \frac{\partial \mu_2(x, y, z, t)}{\partial z} \right] \end{aligned} \quad (3)$$

with boundary and initial conditions

$$\begin{aligned} \left. \frac{\partial \rho(x, y, z, t)}{\partial x} \right|_{x=0} = 0, \quad \left. \frac{\partial \rho(x, y, z, t)}{\partial x} \right|_{x=L_x} = 0, \quad \left. \frac{\partial \rho(x, y, z, t)}{\partial y} \right|_{y=0} = 0, \\ \left. \frac{\partial \rho(x, y, z, t)}{\partial y} \right|_{y=L_y} = 0, \quad \left. \frac{\partial \rho(x, y, z, t)}{\partial z} \right|_{z=0} = 0, \quad \left. \frac{\partial \rho(x, y, z, t)}{\partial z} \right|_{z=L_z} = 0, \end{aligned} \quad (4)$$

$$\rho(x, y, z, 0) = f_V(x, y, z), \quad V(x_1 + V_n t, y_1 + V_n t, z_1 + V_n t, t) = V_\infty \left(1 + 2 \ell \omega / kT \sqrt{x_1^2 + y_1^2 + z_1^2} \right).$$

Here $\rho = I, V$; $I(x, y, z, t)$ is the spatio-temporal distribution of concentration of radiation interstitials; I^* is the equilibrium distribution of interstitials; $D_I(x, y, z, T)$, $D_V(x, y, z, T)$, $D_{IS}(x, y, z, T)$, $D_{VS}(x, y, z, T)$ are the coefficients of volumetric and surficial diffusions of interstitials and vacancies, respectively; terms $V^2(x, y, z, t)$ and $I^2(x, y, z, t)$ correspond to generation of divacancies and diinterstitials, respectively (see, for example, [26] and appropriate references in this book); $k_{I,V}(x, y, z, T)$, $k_{I,I}(x, y, z, T)$ and $k_{V,V}(x, y, z, T)$ are the parameters of recombination of point radiation defects and generation of their complexes; k is the Boltzmann constant; $\omega = a^3$, a is the interatomic distance; ϕ is the specific surface energy. To account porosity of buffer layers we assume, that porous are approximately cylindrical with average values $r = \sqrt{x_1^2 + y_1^2}$ and z_1 before annealing [23]. With time small pores decomposing on vacancies. The vacancies absorbing by larger pores [27]. With time large pores became larger due to absorbing the vacancies and became more spherical [27]. Distribution of concentration of vacancies in heterostructure, existing due to porosity, could be determined by summing on all pores, i.e.

$$V(x, y, z, t) = \sum_{i=0}^l \sum_{j=0}^m \sum_{k=0}^n V_p(x + i\alpha, y + j\beta, z + k\chi, t), \quad R = \sqrt{x^2 + y^2 + z^2}$$

Here α , β and χ are the average distances between centers of pores in directions x , y and z ; l , m and n are the quantity of pores in appropriate directions.

Spatio-temporal distributions of divacancies $\Phi_V(x, y, z, t)$ and diinterstitials $\Phi_I(x, y, z, t)$ could be determined by solving the following system of equations [25, 26].

$$\begin{aligned} \frac{\partial \Phi_\rho(x, y, z, t)}{\partial t} &= \frac{\partial}{\partial x} \left[D_{\Phi_\rho}(x, y, z, T) \frac{\partial \Phi_\rho(x, y, z, t)}{\partial x} \right] + \frac{\partial}{\partial y} \left[D_{\Phi_\rho}(x, y, z, T) \frac{\partial \Phi_\rho(x, y, z, t)}{\partial y} \right] + \\ &+ \frac{\partial}{\partial z} \left[D_{\Phi_\rho}(x, y, z, T) \frac{\partial \Phi_\rho(x, y, z, t)}{\partial z} \right] + \Omega \frac{\partial}{\partial x} \left[\frac{D_{\Phi_\rho S}}{kT} \nabla_s \mu_1(x, y, z, t) \int_0^{L_z} \Phi_\rho(x, y, W, t) dW \right] + \\ &+ \Omega \frac{\partial}{\partial y} \left[\frac{D_{\Phi_\rho S}}{kT} \nabla_s \mu_1(x, y, z, t) \int_0^{L_z} \Phi_\rho(x, y, W, t) dW \right] + k_{\rho, \rho}(x, y, z, T) \rho^2(x, y, z, t) + \\ &+ \frac{\partial}{\partial x} \left[\frac{D_{\Phi_\rho S}}{\bar{V} kT} \frac{\partial \mu_2(x, y, z, t)}{\partial x} \right] + \frac{\partial}{\partial y} \left[\frac{D_{\Phi_\rho S}}{\bar{V} kT} \frac{\partial \mu_2(x, y, z, t)}{\partial y} \right] + \frac{\partial}{\partial z} \left[\frac{D_{\Phi_\rho S}}{\bar{V} kT} \frac{\partial \mu_2(x, y, z, t)}{\partial z} \right] + \\ &+ k_\rho(x, y, z, T) \rho(x, y, z, t) \end{aligned} \quad (5)$$

with boundary and initial conditions

$$\begin{aligned} \left. \frac{\partial \Phi_\rho(x, y, z, t)}{\partial x} \right|_{x=0} &= 0, \quad \left. \frac{\partial \Phi_\rho(x, y, z, t)}{\partial x} \right|_{x=L_x} &= 0, \quad \left. \frac{\partial \Phi_\rho(x, y, z, t)}{\partial y} \right|_{y=0} &= 0, \\ \left. \frac{\partial \Phi_\rho(x, y, z, t)}{\partial y} \right|_{y=L_y} &= 0, \quad \left. \frac{\partial \Phi_\rho(x, y, z, t)}{\partial z} \right|_{z=0} &= 0, \quad \left. \frac{\partial \Phi_\rho(x, y, z, t)}{\partial z} \right|_{z=L_z} &= 0, \end{aligned} \quad (6)$$

$$\Phi_\rho(x, y, z, 0) = f_{\Phi_\rho}(x, y, z).$$

Here $D_{\phi}(x,y,z,T)$, $D_{\phi V}(x,y,z,T)$, $D_{\phi IS}(x,y,z,T)$ and $D_{\phi VS}(x,y,z,T)$ are the coefficients of volumetric and surficial diffusions of complexes of radiation defects; $k_I(x,y,z,T)$ and $k_V(x,y,z,T)$ are the parameters of decay of complexes of radiation defects. Chemical potential μ_1 in Eq.(1) could be determine by the following relation [20].

$$\mu_1 = E(z)\Omega\sigma_{ij} [u_{ij}(x,y,z,t) + u_{ji}(x,y,z,t)]/2, \tag{7}$$

where $E(z)$ is the Young modulus, σ_{ij} is the stress tensor; $u_{ij} = \frac{1}{2}\left(\frac{\partial u_i}{\partial x_j} + \frac{\partial u_j}{\partial x_i}\right)$ is the deformation tensor; u_i, u_j are the components $u_x(x,y,z,t)$, $u_y(x,y,z,t)$ and $u_z(x,y,z,t)$ of the displacement vector $\vec{u}(x,y,z,t)$; x_i, x_j are the coordinate x, y, z . The Eq. (3) could be transform to the following form

$$\begin{aligned} \mu(x,y,z,t) = & \left[\frac{\partial u_i(x,y,z,t)}{\partial x_j} + \frac{\partial u_j(x,y,z,t)}{\partial x_i} \right] \left\{ \frac{1}{2} \left[\frac{\partial u_i(x,y,z,t)}{\partial x_j} + \frac{\partial u_j(x,y,z,t)}{\partial x_i} \right] - \right. \\ & \left. - \varepsilon_0 \delta_{ij} + \frac{\sigma(z)\delta_{ij}}{1-2\sigma(z)} \left[\frac{\partial u_k(x,y,z,t)}{\partial x_k} - 3\varepsilon_0 \right] - K(z)\beta(z)[T(x,y,z,t) - T_0] \delta_{ij} \right\} \frac{\Omega}{2} E(z), \end{aligned}$$

where σ is Poisson coefficient; $\varepsilon_0 = (a_s - a_{EL})/a_{EL}$ is the mismatch parameter; a_s, a_{EL} are lattice distances of the substrate and the epitaxial layer; K is the modulus of uniform compression; β is the coefficient of thermal expansion; T_r is the equilibrium temperature, which coincide (for our case) with room temperature. Components of displacement vector could be obtained by solution of the following equations [21].

$$\begin{cases} \rho(z) \frac{\partial^2 u_x(x,y,z,t)}{\partial t^2} = \frac{\partial \sigma_{xx}(x,y,z,t)}{\partial x} + \frac{\partial \sigma_{xy}(x,y,z,t)}{\partial y} + \frac{\partial \sigma_{xz}(x,y,z,t)}{\partial z} \\ \rho(z) \frac{\partial^2 u_y(x,y,z,t)}{\partial t^2} = \frac{\partial \sigma_{yx}(x,y,z,t)}{\partial x} + \frac{\partial \sigma_{yy}(x,y,z,t)}{\partial y} + \frac{\partial \sigma_{yz}(x,y,z,t)}{\partial z} \\ \rho(z) \frac{\partial^2 u_z(x,y,z,t)}{\partial t^2} = \frac{\partial \sigma_{zx}(x,y,z,t)}{\partial x} + \frac{\partial \sigma_{zy}(x,y,z,t)}{\partial y} + \frac{\partial \sigma_{zz}(x,y,z,t)}{\partial z} \end{cases} \tag{8}$$

Where

$$\sigma_{ij} = \frac{E(z)}{2[1+\sigma(z)]} \left[\frac{\partial u_i(x,y,z,t)}{\partial x_j} + \frac{\partial u_j(x,y,z,t)}{\partial x_i} - \frac{\delta_{ij}}{3} \frac{\partial u_k(x,y,z,t)}{\partial x_k} \right] + K(z)\delta_{ij} \times \frac{\partial u_k(x,y,z,t)}{\partial x_k} - \beta(z)K(z)[T(x,y,z,t) - T_r].$$

$\rho(z)$ is the density of materials of heterostructure, δ_{ij} is the Kronecker symbol. Conditions for the system of Eqs. (8) could be written in the form

$$\frac{\partial \vec{u}(0,y,z,t)}{\partial x} = 0; \frac{\partial \vec{u}(L_x,y,z,t)}{\partial x} = 0; \frac{\partial \vec{u}(x,0,z,t)}{\partial y} = 0; \frac{\partial \vec{u}(x,L_y,z,t)}{\partial y} = 0;$$

$$\frac{\partial \vec{u}(x,y,0,t)}{\partial z} = 0; \frac{\partial \vec{u}(x,y,L_z,t)}{\partial z} = 0; \vec{u}(x,y,z,0) = \vec{u}_0; \vec{u}(x,y,z,\infty) = \vec{u}_0.$$

We calculate spatio-temporal distributions of concentrations of dopant and radiati-on defects by solving the Eqs.(1), (3), (5) and (8) framework standard method of averaging of function corrections [28]. Framework this paper we determine concentration of dopant, concentrations of radiation defects and components of displacement vector by using the second-order approximation framework method of averaging of function corrections. This approximation is usually enough good approximation to make qualitative analysis and to obtain some quantitative results. All obtained results have been checked by comparison with results of numerical simulations.

Discussion

In this section we analyzed dynamics of redistributions of dopant and radiation defects during annealing and under influence of mismatch-induced stress and modification of porosity. Typical distributions of concentrations of dopant in heterostructures are presented on Figs. 2 and 3 for diffusion and ion types of doping, respectively. These distributions have been calculated for the case, when value of dopant diffusion coefficient in doped area is larger, than in nearest areas. The figures show, that inhomogeneity of heterostructure gives us possibility to increase compactness of concentrations of dopants and at the same time to increase homogeneity of dopant distribution in doped part of epitaxial layer. However framework this approach of manufacturing of bipolar transistor it is necessary to optimize annealing of dopant and/or radiation defects. Reason of this optimization is following. If annealing time is small, the dopant did not achieve any interfaces between materials of heterostructure. In this situation one cannot find any modifications of distribution of concentration of dopant. If annealing time is large, distribution of concentration of dopant is too homogenous. We optimize annealing time framework recently introduces approach [29-37]. Framework this criterion we approximate real distribution of concentration of dopant by step-wise function (see Figs. 4 and 5). Farther we determine optimal values of annealing time by minimization of the following mean-squared error

$$U = \frac{1}{L_x L_y L_z} \int_0^{L_x} \int_0^{L_y} \int_0^{L_z} [C(x, y, z, \Theta) - \psi(x, y, z)]^2 dx dy dz, \tag{15}$$

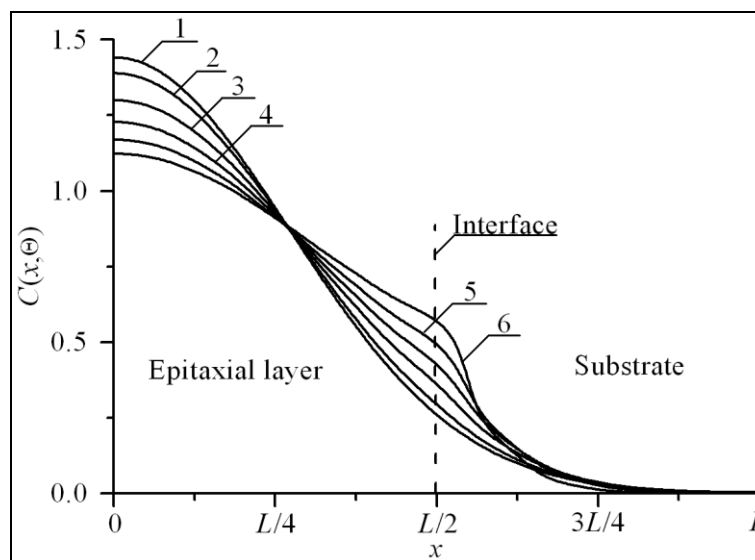


Fig 2: Distributions of concentration of infused dopant in heterostructure

From Fig. 1 in direction, which is perpendicular to interface between epitaxial layer substrate. Increasing of number of curve corresponds to increasing of difference between values of dopant diffusion coefficient in layers of heterostructure under condition, when value of dopant diffusion coefficient in epitaxial layer is larger, than value of dopant diffusion coefficient in substrate.

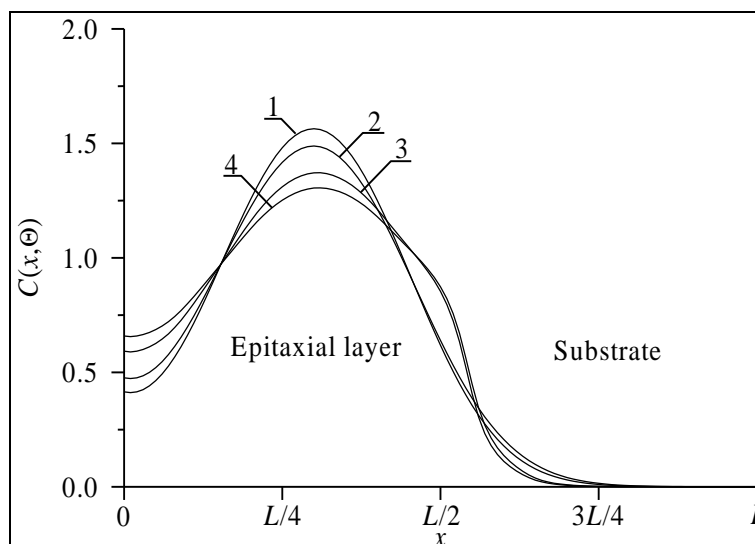


Fig 3: Distributions of concentration of implanted dopant in heterostructure

From Fig. 1 in direction, which is perpendicular to interface between epitaxial layer substrate. Curves 1 and 3 corresponds to annealing time $\Theta = 0.0048(L_x^2+L_y^2+L_z^2)/D_0$. Curves 2 and 4 corresponds to annealing time $\Theta = 0.0057(L_x^2+L_y^2+L_z^2)/D_0$. Curves 1 and 2 corresponds to homogenous sample. Curves 3 and 4 corresponds to heterostructure under condition, when value of dopant diffusion coefficient in epitaxial layer is larger, than value of dopant diffusion coefficient in substrate.

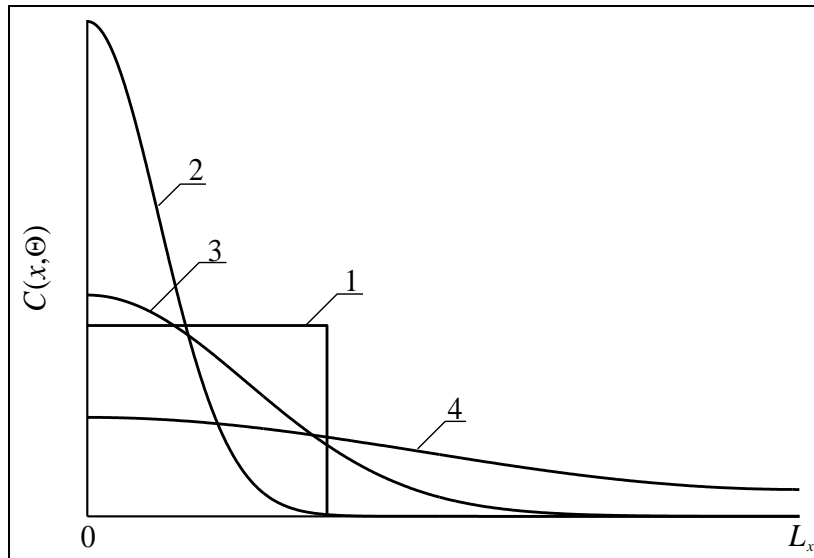


Fig 4: Spatial distributions of dopant in heterostructure after dopant infusion. Curve 1 is idealized distribution of dopant. Curves 2-4 are real distributions of dopant for different values of annealing time. Increasing of number of curve corresponds to increasing of annealing time

where $\psi(x,y,z)$ is the approximation function. Dependences of optimal values of annealing time on parameters are presented on Figs. 6 and 7 for diffusion and ion types of doping, respectively. It should be noted, that it is necessary to anneal radiation defects after ion implantation. One could find spreading of concentration of distribution of dopant during this annealing. In the ideal case distribution of dopant achieves appropriate interfaces between materials of heterostructure during annealing of radiation defects. If dopant did not achieves any interfaces during annealing of radiation defects, it is practicably to additionally anneal the dopant. In this situation optimal value of additional annealing time of implanted dopant is smaller, than annealing time of infused dopant.

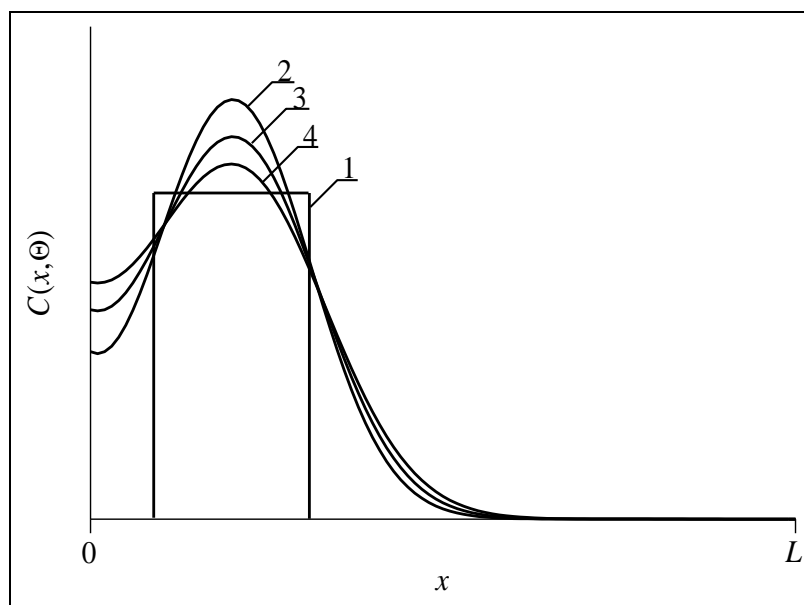


Fig 5: Spatial distributions of dopant in heterostructure after ion implantation. Curve 1 is idealized distribution of dopant. Curves 2-4 are real distributions of dopant for different values of annealing time. Increasing of number of curve corresponds to increasing of annealing time

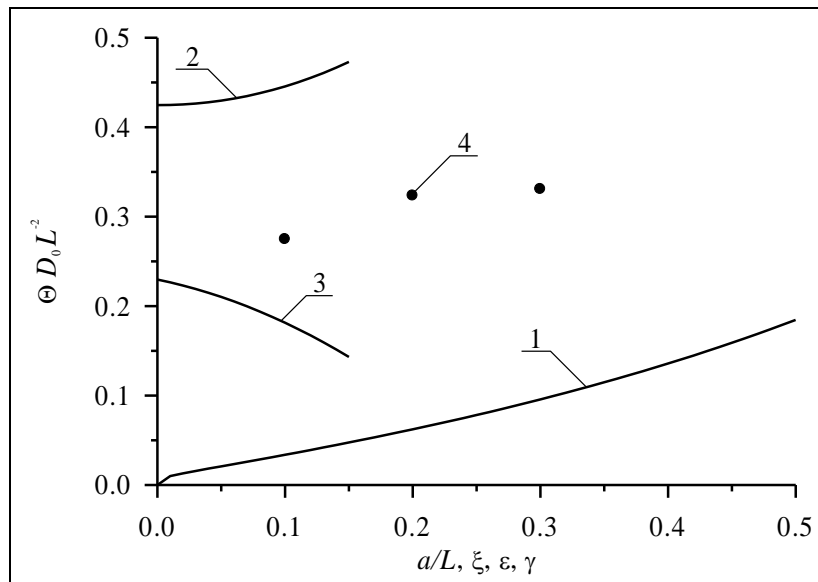


Fig 6: Dependences of dimensionless optimal annealing time for doping by diffusion, which have been obtained by minimization of mean-squared error, on several parameters.

Curve 1 is the dependence of dimensionless optimal annealing time on the relation a/L and $\xi = \gamma = 0$ for equal to each other values of dopant diffusion coefficient in all parts of heterostructure. Curve 2 is the dependence of dimensionless optimal annealing time on value of parameter ε for $a/L=1/2$ and $\xi = \gamma = 0$. Curve 3 is the dependence of dimensionless optimal annealing time on value of parameter ξ for $a/L=1/2$ and $\varepsilon = \gamma = 0$. Curve 4 is the dependence of dimensionless optimal annealing time on value of parameter γ for $a/L=1/2$ and $\varepsilon = \xi = 0$

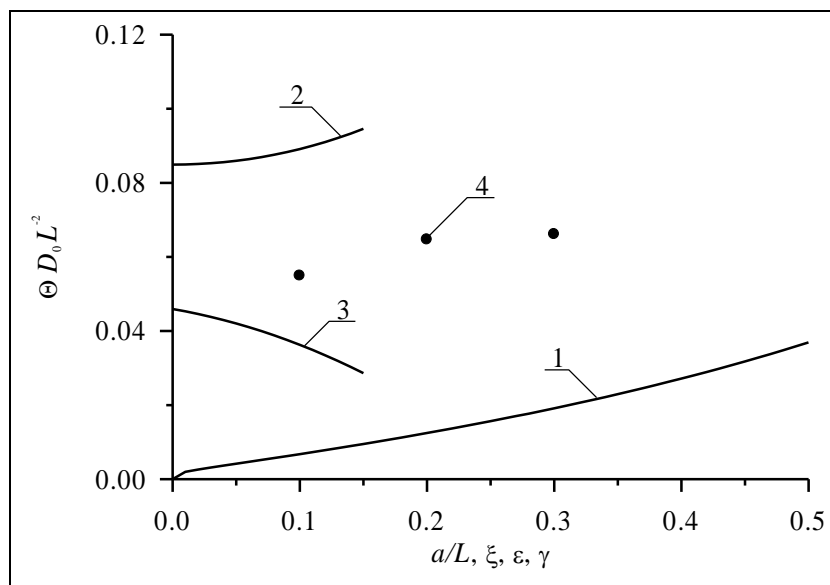


Fig 7: Dependences of dimensionless optimal annealing time for doping by ion implantation, which have been obtained by minimization of mean-squared error, on several parameters.

Curve 1 is the dependence of dimensionless optimal annealing time on the relation a/L and $\xi = \gamma = 0$ for equal to each other values of dopant diffusion coefficient in all parts of heterostructure. Curve 2 is the dependence of dimensionless optimal annealing time on value of parameter ε for $a/L=1/2$ and $\xi = \gamma = 0$. Curve 3 is the dependence of dimensionless optimal annealing time on value of parameter ξ for $a/L=1/2$ and $\varepsilon = \gamma = 0$. Curve 4 is the dependence of dimensionless optimal annealing time on value of parameter γ for $a/L=1/2$ and $\varepsilon = \xi = 0$

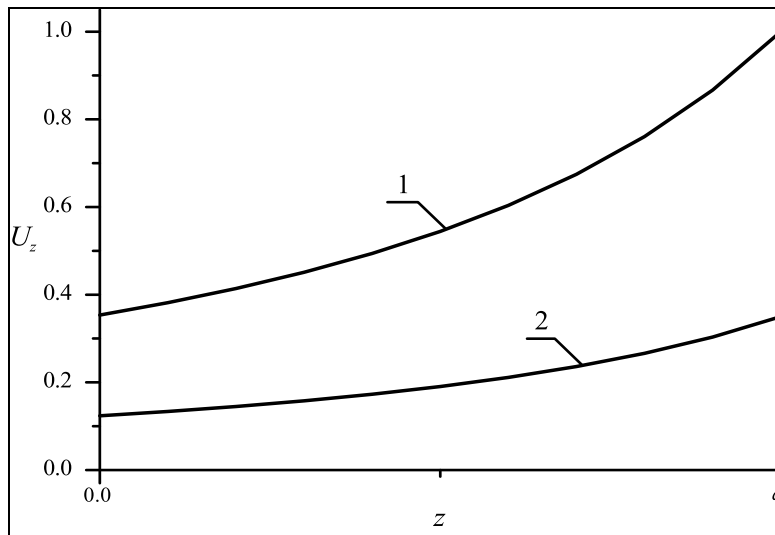


Fig 8: Normalized dependences of component u_z of displacement vector on coordinate z for nonporous (curve 1) and porous (curve 2) epitaxial layers

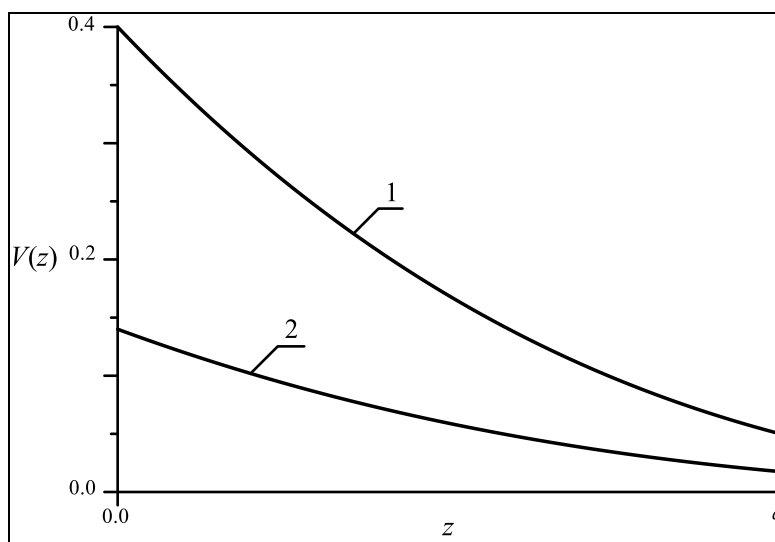


Fig 9: Normalized dependences of vacancy concentrations on coordinate z in unstressed (curve 1) and stressed (curve 2) epitaxial layers

Farther we analyzed influence of relaxation of mechanical stress on distribution of dopant in doped areas of heterostructure. Under following condition $\varepsilon_0 < 0$ one can find compression of distribution of concentration of dopant near interface between materials of heterostructure. Contrary (at $\varepsilon_0 > 0$) one can find spreading of distribution of concentration of dopant in this area. This changing of distribution of concentration of dopant could be at least partially compensated by using laser annealing^[37]. This type of annealing gives us possibility to accelerate diffusion of dopant and another processes in annealed area due to inhomogenous distribution of temperature and Arrhenius law. Accounting relaxation of mismatch-induced stress in heterostructure could leads to changing of optimal values of annealing time. At the same time modification of porosity gives us possibility to decrease value of mechanical stress. On the one hand mismatch-induced stress could be used to increase density of elements of integrated circuits. On the other hand could leads to generation dislocations of the discrepancy. Figs. 8 and 9 show distributions of concentration of vacancies in porous materials and component of displacement vector, which is perpendicular to interface between layers of heterostructure.

Conclusion

In this paper we model redistribution of infused and implanted dopants with account relaxation mismatch-induced stress during manufacturing field-effect heterotransistors framework a differential-drive CMOS rectifier. We formulate recommendations for optimization of annealing to decrease dimensions of transistors and to increase their density. We formulate recommendations to decrease mismatch-induced stress. Analytical approach to model diffusion and ion types of doping with account concurrent changing of parameters in space and time has been introduced. At the same time the approach gives us possibility to take into account nonlinearity of considered processes.

References

1. Lachin VI, Savelov NS. *Electronics*. Rostov-on-Don: Phoenix, 2001.
2. Polishcuk A. *Modern Electronics*. 2004;12:8-11.

3. Volovich G. *Modern Electronics*. 2006;2:10-17.
4. Kerentsev A, Lanin V. *Power Electronics*. 2008;1:34.
5. Ageev AO, Belyaev AE, Boltovets NS, Ivanov VN, Konakova RV, Kudrik Ya Ya, Litvin PM, *et al.* *Semiconductors*. 2009;43(7):897-903.
6. Jung-Hui Tsai, Shao-Yen Chiu, Wen-Shiung Lour, Der-Feng Guo. *Semiconductors*. 2009;43(7)C:971-974.
7. Alexandrov OV, Zakhar'in AO, Sobolev NA, Shek EI, Makoviychuk MM, Parshin EO. *Semiconductors*. 1998;32(9):1029-1032.
8. Ermolovich IB, Milenin VV, Red'ko RA, Red'ko SM. *Semiconductors*. 2009;43(8):1016-1020.
9. Sinsermsuksakul P, Hartman K, Kim SB, Heo J, Sun L, Park HH, *et al.* *Appl. Phys. Lett.* 2013;102(5):053901-053905.
10. Reynolds JG, Reynolds CL Jr, Mohanta A, Muth JF, Rowe JE, Everitt HO, *et al.* *Appl. Phys. Lett.* 2013;102(15):152114-152118.
11. Volokobinskaya NI, Komarov IN, Matyukhina TV, Reshetnikov VI, Rush AA, Falina IV, *et al.* *Semiconductors*. 2001;35(8):1013-1017.
12. Pankratov EL, Bulaeva EA. *Reviews in Theoretical Science*. 2013;1(1):58-82.
13. Kukushkin SA, Osipov AV, Romanychev AI. *Physics of the Solid State*. 2016;58(7):1448-1452.
14. Trukhanov EM, Kolesnikov AV, Loshkarev ID. *Russian Microelectronics*. 2015;44(8):552-558.
15. Pankratov EL, Bulaeva EA. *Reviews in Theoretical Science*. 2015;3(4):365-398.
16. Ong KK, Pey KL, Lee PS, Wee ATS, Wang XC, Chong YF. *Appl. Phys. Lett.* 2006;89(17):172111-172114.
17. Wang HT, Tan LS, Chor EF. *J. Appl. Phys.* 2006;98(9):094901-094905.
18. Yu V, Bykov AG, Yermeev NA, Zharova IV, Plotnikov KI, Rybakov MN, *et al.* *Radiophysics and Quantum Electronics*. 2003;43(3):836-843.
19. Chang Y, Chouhan SS, Halonen K. *Analog. Integr. Circ. Sig. Process.* 2017;90:113-124.
20. Zhang YW, Bower AF. *Journal of the Mechanics and Physics of Solids*. 1999;47(11):2273-2297.
21. Landau LD, Lifshits EM. *Theoretical physics. 7 (Theory of elasticity)* Physmatlit, Moscow, 2001.
22. Kitayama M, Narushima T, Carter WC, Cannon RM, Glaeser AM. *J. Am. Ceram. Soc.* Vol. 83. P. 2561 (2000); M. Kitayama, T. Narushima, A.M. Glaeser. *J. Am. Ceram. Soc.* 2000;83:2572.
23. Cheremskoy PG, Slesov VV, Betekhtin VI. *Pore in solid bodies*, Energoatomizdat, Moscow, 1990.
24. Yu Z. *Gotra, Technology of microelectronic devices, Radio and communication*, Moscow, 1991.
25. Fahey PM, Griffin PB, Plummer JD. *Rev. Mod. Phys.* 1989;61(2):289-388.
26. Vinetskiy VL, Kholodar' GA. *Radiative physics of semiconductors*. Naukova Dumka, Kiev, 1979.
27. Mynbaeva MG, Mokhov EN, Lavrent'ev AA, Mynbaev KD. *Techn. Phys. Lett.* 2008;34(17):13.
28. Yu Sokolov D. *Applied Mechanics*. 1955;1(1):23-35.
29. Pankratov EL. *Russian Microelectronics*. 2007;36(1):33-39.
30. Pankratov EL. *Int. J. Nanoscience*. 2008;7(4-5):187-197.
31. Pankratov EL, Bulaeva EA. *Reviews in Theoretical Science*. 2013;1(1):58-82.
32. Pankratov EL, Bulaeva EA. *Int. J. Micro-Nano Scale Transp.* 2012;3(3):119-130.
33. Pankratov EL, Bulaeva EA. *International Journal of Modern Physics B*. 2015;29(5):1550023-1-1550023-12.
34. Pankratov EL. *J. Comp. Theor. Nanoscience*. 2017;14(10):4885-4899.
35. Pankratov EL, Bulaeva EA. *Materials science in semiconductor processing*. 2015;34:260-268.
36. Pankratov EL, Bulaeva EA. *Int. J. Micro-Nano Scale Transp.* 2014;4(1):17-31.
37. Pankratov EL. *Nano*. 2011;6(1):31-40.